Perth Hydro

Level 29, 221 St Georges Tce
Perth, WA 6000

Contact: Dr Tim Gourlay
+61 416 328883
tim@perthhydro.com

# Double-Humped Roll Response for a Cruise Ship in Beam Seas

Tim Gourlay

Perth Hydro Research Report R2022-03

Presented to the Royal Institution of Naval Architects, Fremantle, 14th December 2022

| Document History | |
|---|---|
| 14 December 2022 | Report published |

## SUMMARY

A set of model tests was published by Ikeda and other authors in 2006, for a Fincantieri cruise ship in regular beam seas of height 5.0 m, with varying wave period. They made the unexpected discovery of a “double-humped” roll response, with one hump at the resonant roll period of 23 seconds, and another hump at short wave periods of 7 – 11 seconds, where the wave-induced roll moment is largest. The hump at the resonant roll period is predicted by linear theory, but the hump at short wave periods is not. In this article, we show that including nonlinear effects on the GZ curve, including heave and position in the wave, allows the second roll peak to be predicted. The implication is that for low-GM ships in short-period waves, linear roll theory may be inadequate, and a nonlinear theory may be needed.

## CONTENTS



## NOMENCLATURE

| | |
|---|---|
| AP | Aft perpendicular |
| $B_{WL}$ | Waterline beam |
| GM | Transverse metacentric height above centre of gravity |
| KG | Centre of gravity height above keel |
| KM | Transverse metacentric height above keel |
| LBP | Length between perpendiculars |
| LCB | Longitudinal centre of buoyancy |
| LOA | Length overall |
| RAO | Response amplitude operator |

## 1. Introduction

Ikeda et al. (2006) describe a set of model tests on a generic Fincantieri cruise ship hull. The tests were done in the towing tank of Osaka Prefecture University, with the ship free to heave, sway, roll and pitch. Roll motions were measured in regular beam seas, of constant full-scale height 5.0 m and varying wave period. Results are shown in Figure 1, for the ship without bilge keels.

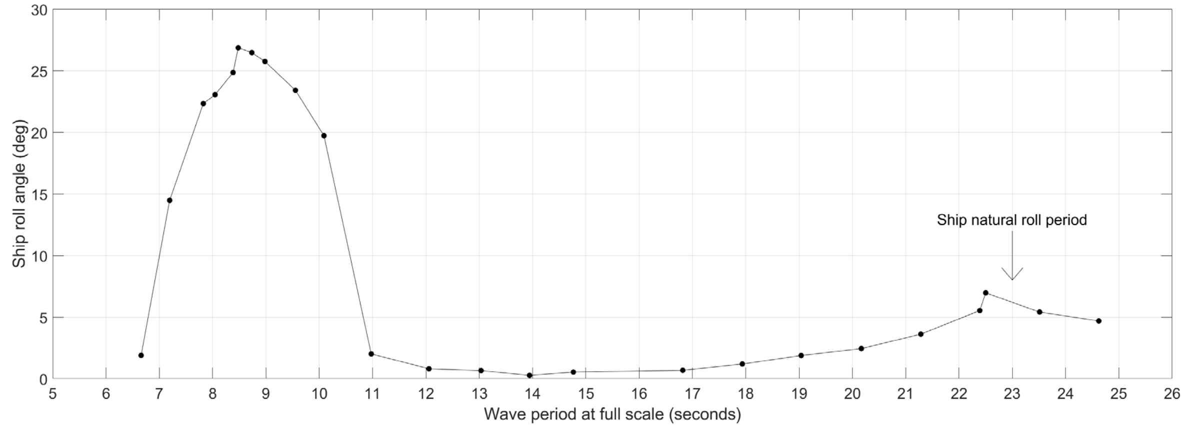


**Figure 1: Measured roll angle of Fincantieri cruise ship hull, in regular beam seas of height 5.0 m. Data from Ikeda et al. (2006, Fig. 2) and Munif et al. (2005, Fig. 3).**

For the large-wave conditions shown in Figure 1, the roll has a peak at the ship’s natural roll period of 23 seconds, as expected. However, it also has another (much larger) peak at the short wave period of 8.5 seconds. As we shall see, this peak is not predicted by linear seakeeping theory. It is the purpose of this article to investigate the possible nonlinear effects which might produce this large roll peak at short wave periods.

## 2. Hull modelling

The ship hull used in the model tests of Ikeda et al. (2006) was a small-scale model of the Fincantieri standard cruise ship hull (IMO 2004, pp. 19-20). A body plan of the hull is given in Ikeda et al. (2006) and Munif et al. (2006).

A larger-scale model of the same hull is shown in Figure 2.

Figure 2: 1:40 scale model of Fincantieri standard cruise ship hull, as tested at Vienna Model Basin (from IMO 2004, p. 22)

Dimensions of the model tested by Ikeda et al. (2006) are shown in Table 1.

| Supplied hull details | |
|---|---|
| Model scale | 1 : 125.32 |
| LOA | 290.0 m |
| LBP | 242.24 m |
| $B_{WL}$ | 36.0 m |
| Depth | 20.0 m |
| Draft | 8.4 m |
| Displacement | 53,140 tonnes |
| Block coefficient | 0.709 |
| GM | 1.58 m |
| Natural roll period | 23 seconds |

Table 1: Details of Fincantieri standard cruise ship, as tested by Ikeda et al. (2006). All dimensions given at full scale.

A surface mesh of the hull, suitable for hydrostatics calculations, has been developed from the supplied body plan. This is shown in Figure 3.

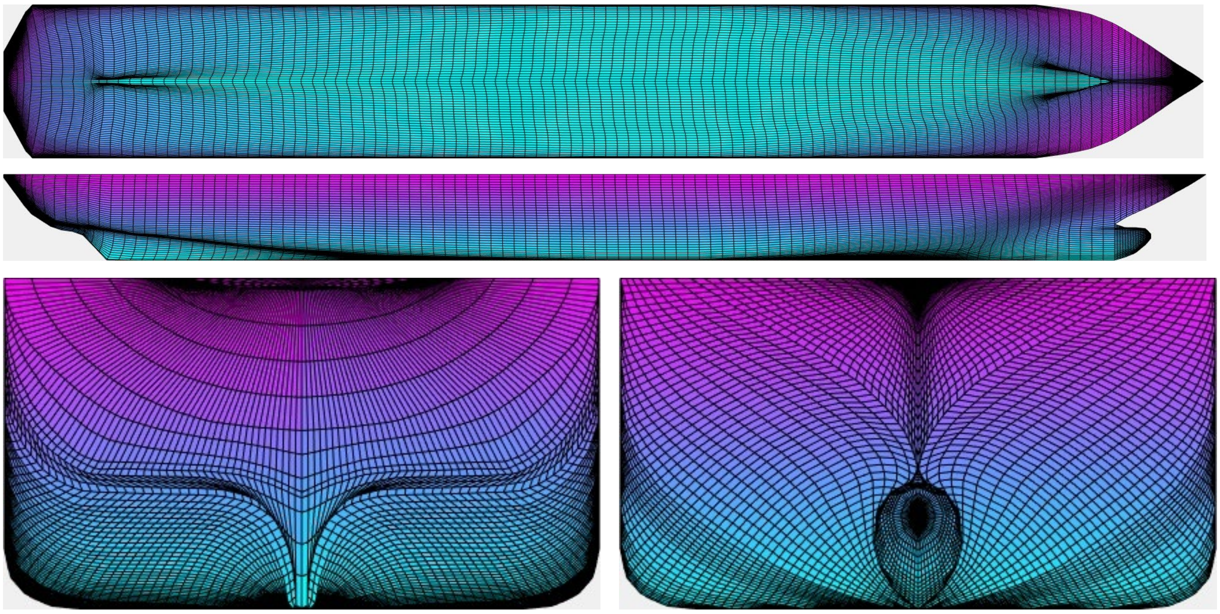

Figure 3: 14048-panel surface mesh, up to deck level, as developed with OCTOPUS 3D Mesher for hydrostatics calculations

Another (coarser) surface mesh of the hull, up to the still waterline, has been developed for seakeeping calculations. This is shown in Figure 4.

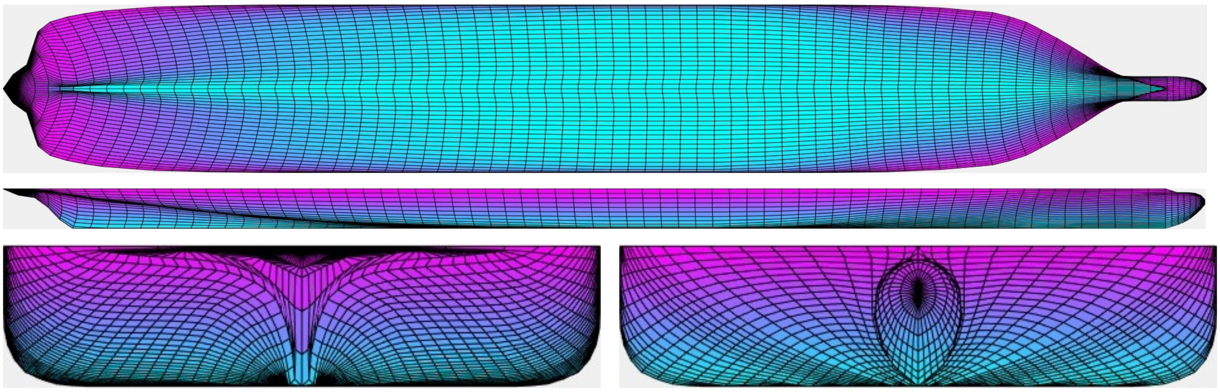

Figure 4: 3780-panel surface mesh, up to still waterline, as developed with OCTOPUS 3D Mesher for seakeeping calculations

From the developed surface meshes, stability parameters have been calculated, as shown in Table 2.

| Calculated stability parameters | |
|---|---|
| KM | 20.00 m |
| KG = KM-GM | 18.42 m |
| LCB | 119.4 m forward of AP |

Table 2: Calculated stability parameters

## 3. Linear frequency-domain calculations

Linear beam-sea ship roll was first calculated in the frequency domain. Wave loads, ship hydrodynamic coefficients and ship RAOs were calculated using WAMIT v7.4 software (WAMIT 2020). This software has been validated against beam-sea model test results in low wave conditions, in a previous study with DNV and Flanders Hydraulics (Gourlay et al. 2015).

We use a coordinate system with origin at the ship's LCG (119.4 m forward of the AP), on the ship centreline, and on the still waterline. Roll moments are taken about this origin. The vertical centre of gravity is 10.02 m above this origin (from Table 2).

In this report, we shall use the following nomenclature for the six motion degrees of freedom:
$x_1$= "surge" (fore-aft motion at ship origin, positive forward)
$x_2$ = "sway" (transverse motion at ship origin, positive to port)
$x_3$ = "heave" (vertical motion at ship origin, positive upwards)
$x_4$ = "roll" (angle, positive to starboard)
$x_5$ = "pitch" (angle, positive bow-down)
$x_6$ = "yaw" (angle, positive bow-to-port).

Roll motions are coupled with sway and yaw motions, but are uncoupled from surge, heave and pitch motions in the linear case. Nevertheless, we solve for the full 6-DoF motions, to prepare for the nonlinear analysis.

WAMIT settings for frequency-domain calculations are shown in Table 3.

| **WAMIT settings – frequency domain** | |
|---|---|
| WAMIT solver | Direct solver |
| First-order wave loads | Diffraction potential, 6-DoF |
| Added mass and damping | Radiation potential, coupled 6-DoF |
| Restoring coefficients | Standard WAMIT upright hydrostatics |
| Force control method | Force control 2 with external damping |
| Water depth | Deep water |
| Ship speed | 0 knots |
| Ship heading relative to waves | 90º (starboard beam seas) |
| Wave periods | 5.0 : 0.05 : 26.0 seconds |
| Roll gyradius | 43% of waterline beam (tuned to correct roll period) |
| Viscous roll damping | Linear Ikeda method for eddy damping (Ikeda et al., 1978) |
| Pitch gyradius | 25% of LOA |
| Yaw gyradius | 25% of LOA |

Table 3: WAMIT settings for frequency-domain calculations

The wave-induced roll moment, as a function of wave frequency, is shown in Figure 5. Sway and yaw wave loads are also calculated and included in the modelling.

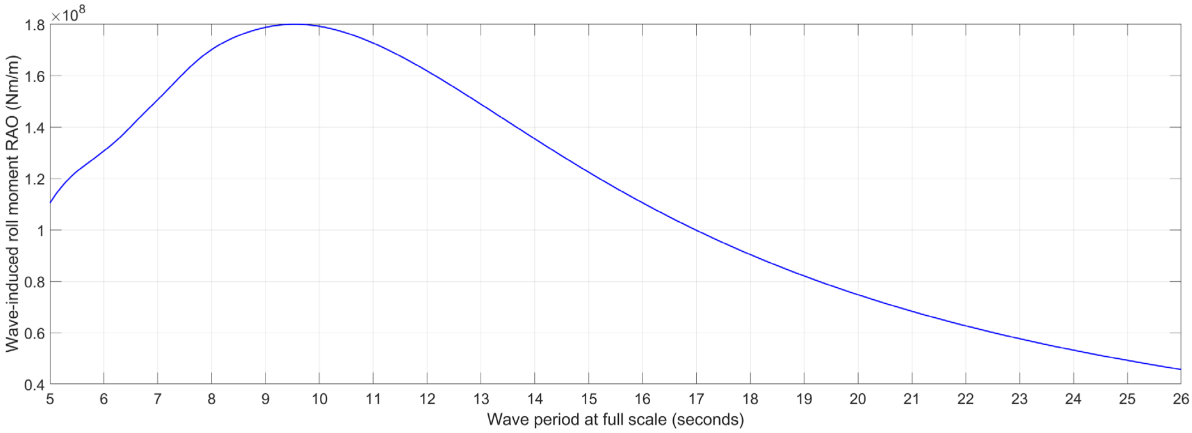


**Figure 5: Wave-induced roll moment, per metre of wave amplitude, as a function of wave period**

Roll added inertia and damping, as a function of wave frequency, are shown in Appendix A. Cross-coupling terms with sway and yaw are also calculated and included in the modelling.

The roll restoring coefficient is shown in Table 4. There are no cross-coupling restoring coefficients for roll.

| | |
|---|---|
| $C_{44}$ | 8.24 x $10^8$ Nm |

**Table 4: Linear roll restoring coefficient**

## 4. Linear time-domain calculations

Time-domain motions were calculated using a fourth-order Runge-Kutta solver, as implemented in the software MoorMotions (www.moormotions.com). The method solves for displacements, velocities and accelerations in multiple coupled degrees of freedom, using any input forcing functions.

The basic time-domain equation to be solved is (van Oortmerssen 1974 eq. 4.23, Gourlay 2019 eq. 1)

$$\sum_{j=1}^{6}[M_{ij} + A_{ij}(\infty)]\ddot{x}_j = X_i - C_i - B_{iV} - \int_0^{\infty}\sum_{j=1}^{6} L_{ij}(\tau)\ddot{x}_j(t-\tau)d\tau \qquad (1)$$

The symbols are defined as follows:
$x_j$= motion in each degree of freedom, $j = 1, \ldots, 6$
$M_{ij}$ = mass matrix
$A_{ij}(\infty)$ = added mass at infinite frequency
$X_i$ = wave load
$C_i$ = hydrostatic restoring force
$B_{iV}$ = viscous damping force
$L_{ij}(\tau)$ = acceleration-based impulse response functions

Wave loads are calculated using WAMIT, as for the frequency-domain calculations.

For time-domain calculations, time-domain impulse response functions (Gourlay 2021) are used, instead of frequency-domain added mass and damping. Impulse response functions are calculated using WAMIT, as shown in Table 5.

| WAMIT settings – impulse response functions | |
|---|---|
| Wave frequencies | 0.00 : 0.01 : 5.00 rad/s, plus infinite frequency |
| Impulse response function method | WAMIT f2t utility, coupled 6-DoF |
| Time step | 0.1 seconds |
| Time duration | 60 seconds |

**Table 5: WAMIT settings for impulse response functions**

The roll impulse response function is shown in Appendix A. Cross-coupling terms with sway and yaw are also calculated and included in the modelling.

Equation (1) is solved for regular waves of varying input frequency, with height 5.0 m, using the MoorMotions time-domain solver. Inputs are described in Table 7.

| MoorMotions inputs – linear time-domain calculations | |
|---|---|
| $M_{ij}$ | WAMIT (2019, eq. 3.3), as used in frequency-domain |
| $X_i$ | Output from WAMIT, as used in frequency-domain |
| $C_i$ | Output from WAMIT, as used in frequency-domain |
| $B_{iV}$ | Linear eddy roll damping, as used in frequency-domain |
| $L_{ij}(\tau)$ | Output from WAMIT for time-domain calculations |
| $A_{ij}(\infty)$ | Output from WAMIT for time-domain calculations |
| Simulation timestep | 0.1 seconds |
| Simulation time | 900 seconds |
| Wave ramp-up time | 300 seconds |

**Table 6: MoorMotions inputs for linear time-domain calculations**

## 5. Nonlinear time-domain calculations

For nonlinear time-domain calculations, we use the nonlinear roll righting moment, rather than the linearized roll restoring coefficient shown in Table 4. The roll righting moment is related to the ship mass $m$, acceleration due to gravity $g$ and righting lever $GZ$ by

$$C_4 = m.g.GZ \tag{2}$$

In still water, the GZ curve can be calculated by applying hydrostatic pressure to the heeled hull surface mesh. The calculated still-water GZ curve is shown in Figure 8, up to 30˚ heel angle. The heel angle for deck edge immersion is 33˚.

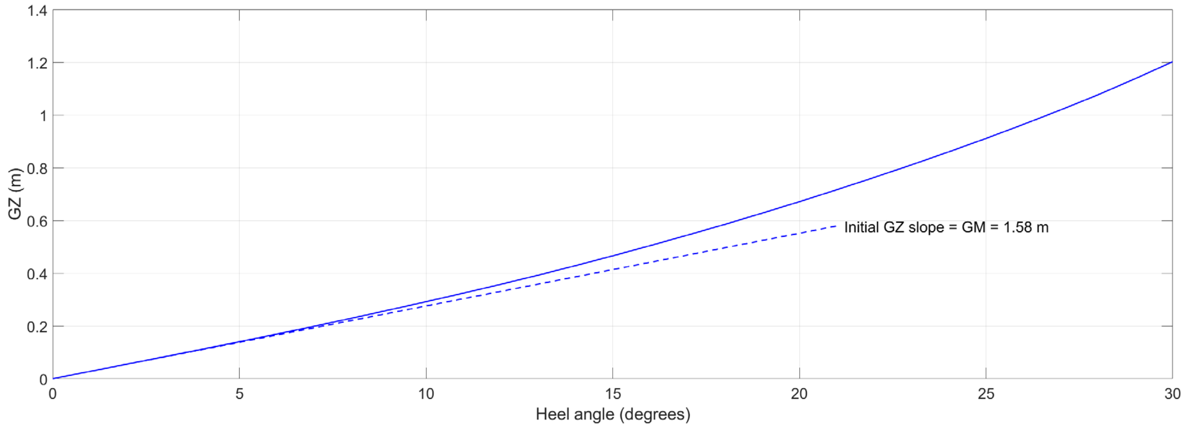


**Figure 6: Calculated still-water GZ curve for the Fincantieri hull model**

In a nonlinear analysis, we can also account for the changing righting moment with position in the wave. Example calculated GZ curves for 8.5 second waves are shown in Figure 8. Results are plotted for different heave values: zero heave and equilibrium heave (as shown in Figure 7).

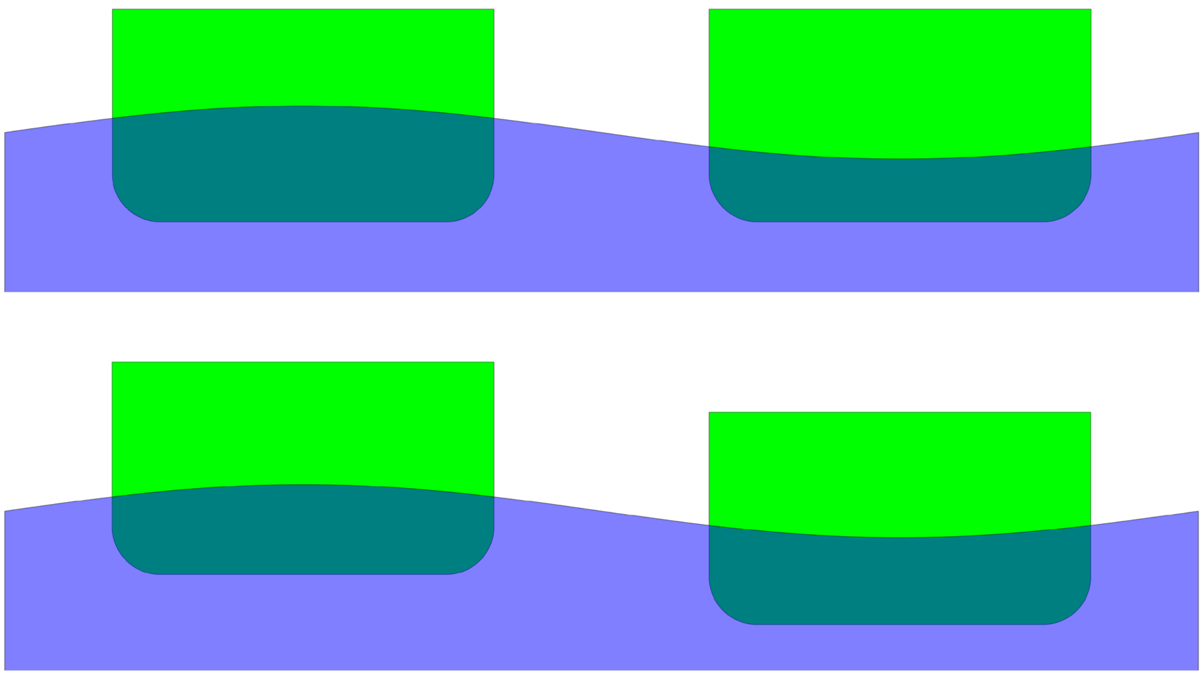

**Figure 7: Stern view of cruise ship in beam seas, showing submerged hull in crest and trough. Wave height = 5.0 m, wave period = 8.5 seconds. (Top) Zero heave. (Bottom) Buoyancy equilibrium heave.**

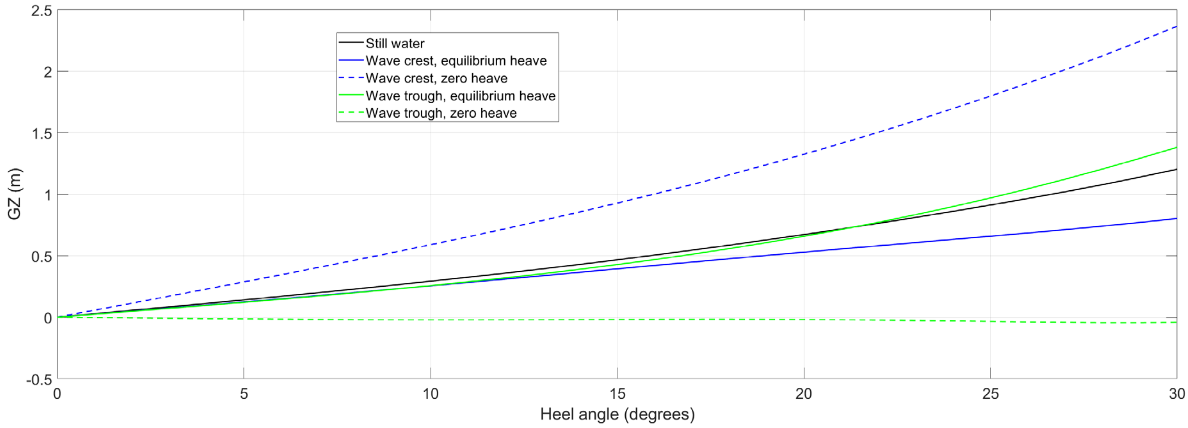


**Figure 8: Righting lever curve for cruise ship in beam seas of height 5.0 m and period 8.5 seconds. Results are given for the ship in the wave crest or wave trough, and with zero heave or buoyancy equilibrium heave.**

In a linear analysis, roll is coupled with sway and yaw, while heave is coupled with surge and pitch. In the nonlinear analysis, we see that ship heave affects the righting moment, so roll is coupled with heave. Therefore, in a nonlinear analysis, all 6-DoF motions are coupled.

We now proceed to solve equation (1) for regular waves of varying input frequency, with height 5.0 m, using the MoorMotions time-domain solver. Inputs are as described in Table 6, with modifications shown in Table 7.

| **Modified MoorMotions inputs for nonlinear time-domain calculations** | |
|---|---|
| $C_4$ | Output from hydrostatic calculations, using instantaneous roll, heave and position in wave |
| $B_{iV}$ | Quadratic eddy roll damping (Ikeda et al. 1978) |

**Table 7: Modified MoorMotions inputs for nonlinear time-domain calculations**

Example ship motion timeseries are shown in Figure 9.

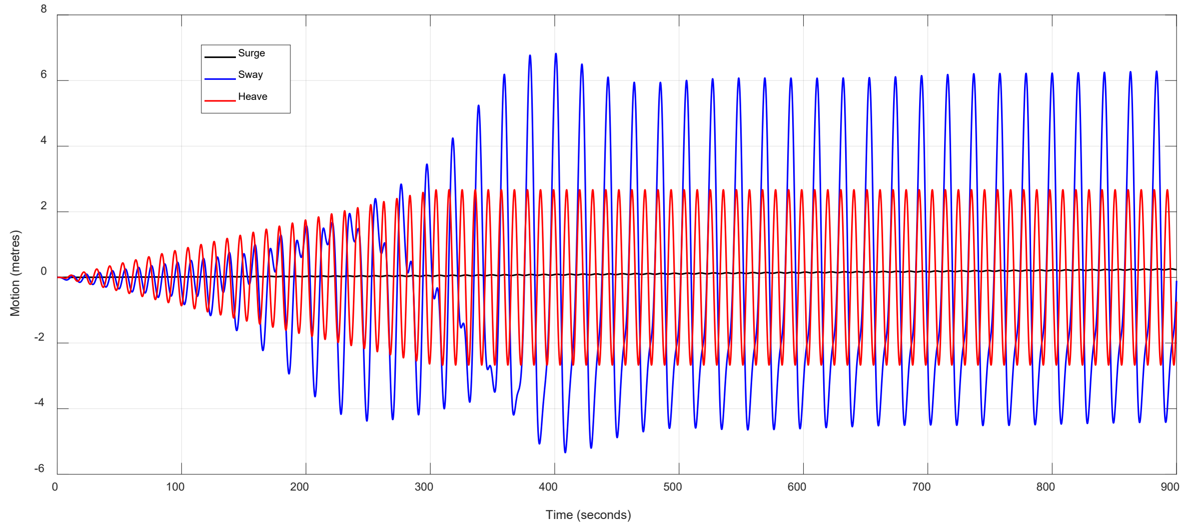


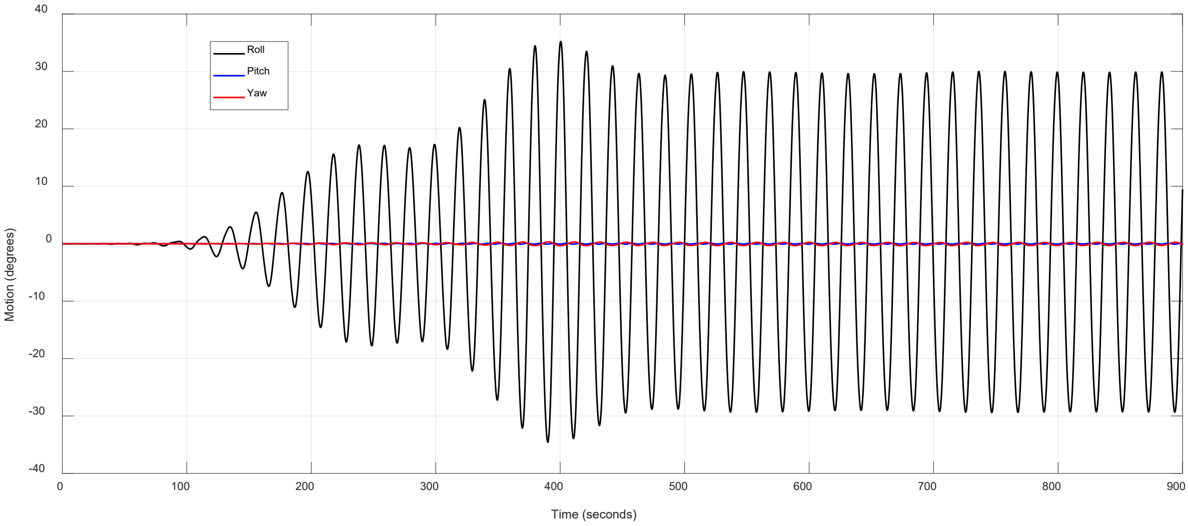


**Figure 9: Calculated nonlinear time-domain motions for the Ikeda et al. (2006) test case, 5.0 m beam seas with period 10.5 seconds. (Top) heave; (Bottom) roll.**

## 6. Comparison of different methods with model tests

Peak roll amplitude results for each wave frequency are shown in Figure 10, together with measured results.

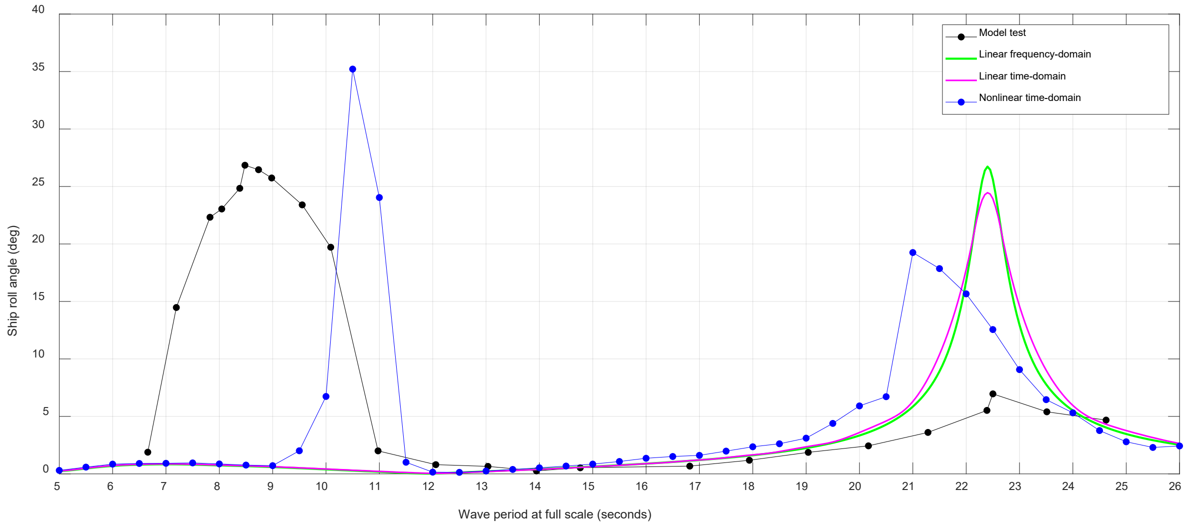


**Figure 10: Comparison of measured and computed ship roll motions, for the Ikeda et al. (2006) test case: cruise ship in regular beam seas of height 5.0 m**

Points to note from Figure 10 include:

- The linear frequency-domain and linear time-domain methods produce near-identical results (see also Figure 11). This is a useful validation of the MoorMotions time-domain solver and impulse response functions.
- The linear and nonlinear theories all predict the approximate location of the resonant roll peak, at 21 – 24 seconds.
- The magnitude of the resonant roll peak is over-predicted. The resonant roll peak is very sensitive to the roll damping. It is likely that the viscous roll damping is under-predicted, perhaps due to the inapplicability of the Ikeda roll damping method to this hull.
- The linear methods completely fail to predict the short-period roll peak, at 7 – 11 seconds.
- The nonlinear method does predict a short-period roll peak, at 9 – 12 seconds. This roll peak is driven by the large wave-induced roll moment at these wave periods (see Figure 5), which is able to excite roll motions at the resonant frequency, primarily through the nonlinear GZ curve.
- Regular waves with 10 second period are able to produce resonant roll with 23 second period, through nonlinear excitation. This is shown numerically in Figure 9, and experimentally in Ikeda et al. (2006, Fig. 5).

As an aside, the heave motions appear unaffected by nonlinear roll behaviour, with the linear and nonlinear methods giving nearly identical heave motions (Figure 11). This confirms the general view that heave may be well-predicted by linear seakeeping theory.

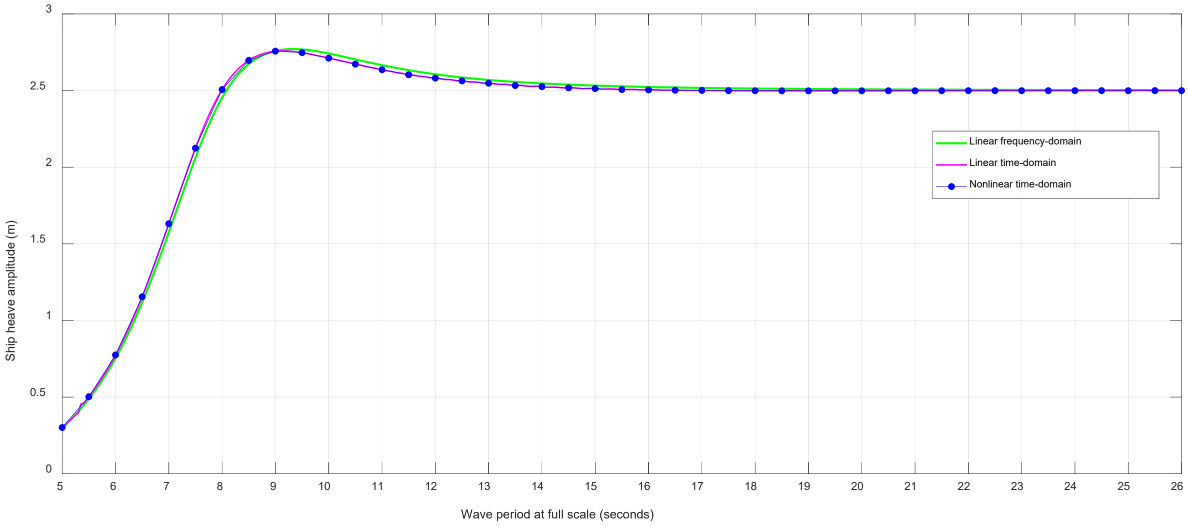


**Figure 11: Computed ship heave, for the Ikeda et al. (2006) test case**

# 7. Effect of bilge keels

The model test results shown in Figure 1 were measured without bilge keels. Further tests were done on the same ship with bilge keels, showing much lower roll motions at the 7 – 11 second peak. We conclude that roll damping is very important for this secondary roll peak.

# 8. Relevant full-scale measurements on container ships

Full-scale roll measurements were done on container ships in beam seas, as reported in Ha & Gourlay (2018, Fig. 11). It was found that for Post-Panamax ships with shorter natural roll periods, RMS roll motions were well-predicted by linear theory. However, for Panamax ships with long natural roll periods of 20 – 30 seconds, linear theory under-predicted the RMS roll motions.

# 9. A warning on predicting roll motions of low-GM ships

Certain classes of ship have large displacement, combined with low transverse GM, resulting in long natural roll periods in the range 20 – 30 seconds. The cruise ship considered in this report fits into this category, as do Panamax container ships and fully-loaded LNG carriers.

Wave conditions around the globe typically have periods in the range 5 – 15 seconds (though sometimes longer).

Let us consider the case of a Panamax container ship, with natural roll period of 25 seconds, in irregular beam seas of peak period 12 seconds. A standard linear seakeeping analysis would calculate a roll RAO with peak at 25 seconds, and tiny RAO at 12 seconds. A measured wave spectrum in this case would have a peak at 12 seconds, and tiny wave energy at 25 seconds. Multiplying the RAO by the wave spectrum, in a standard convolution analysis, produces a tiny roll response. As discussed for the container ship full-scale trials above, this is incorrect.

Therefore, in either regular or irregular beam seas, care must be taken when the ship's natural roll period is much larger than the peak wave period. In this case, linear theory should be expected to under-predict the roll motions, while a fully-nonlinear theory should provide a better prediction.

## 10. Conclusions

For the cruise ship without bilge keels tested by Ikeda et al. (2006), a double-humped roll response was found to occur. This cannot be predicted by linear seakeeping theory, but can be predicted by nonlinear seakeeping theory.

The implication is that for low-GM ships such as cruise ships, container ships and LNG carriers, care should be taken when predicting roll motions using linear theory.

## 11. References

Gourlay, T.P., von Graefe, A., Shigunov, V., Lataire, E. (2015) Comparison of AQWA, GL RANKINE, MOSES, OCTOPUS, PDSTRIP and WAMIT with model test results for cargo ship wave-induced motions in shallow water. Proceedings, 34th International Conference on Ocean, Offshore and Arctic Engineering, St. John's, Canada.

Gourlay, T.P. (2021) Calculation of hydrodynamic impulse response functions using Filon quadrature. Perth Hydro Research Report R2021-05.

Gourlay, T.P. (2019) Comparison of WAMIT and MoorMotions with model tests for a tanker moored at an open berth. Perth Hydro Research Report R2019-09.

Ha, J.-H., Gourlay, T.P. (2018) Full-scale measurements and method validation of container ship wave-induced motions at the Port of Fremantle. Journal of Waterway, Port, Coastal and Ocean Engineering, Vol. 144, No. 6.

Ikeda, Y., Munif, A., Katayama, T., Fujiwara, T. (2006) Large parametric rolling of a large passenger ship in beam seas and the role of bilge keel in its restraint. Marine Systems and Ocean Technology, Vol. 2, No. 1-2.

Ikeda, Y., Himeno, Y., Tanaka, N. (1978) On eddy making of roll damping force on naked hull. Osaka Prefecture University, Department of Naval Architecture, Report No. 00403.

International Maritime Organization (2004) Development of revised SOLAS, Chapter II-1 Parts A, B and B-1, Damage stability probabilistic approach, SAFENVSHIP extension research activities, submitted by Italy.

Munif, A., Katayama, T., Ikeda, Y. (2005) Numerical prediction of parametric rolling of a large passenger ship in beam seas. Conference proceedings of the Japan Society of Naval Architects and Ocean Engineers, No. 1.

Munif, A., Ikeda, Y., Fujiwara, T., Katayama, T. (2006) Parametric roll resonance of a large passenger ship in dead ship condition in all heading angles. Proceedings of the 9th International Conference on Stability of Ships and Ocean Vehicles (STAB2006).

Van Oortmerssen, G. (1973) The motions of a moored ship in waves. Netherlands Ship Model Basin, Publication No. 510.

WAMIT (2020) WAMIT v7.4 User Manual. WAMIT Inc.

# Appendix A – Calculation of impulse response functions

Frequency-domain added inertia and damping coefficients for roll, as calculated using WAMIT, are shown in Figure 12.

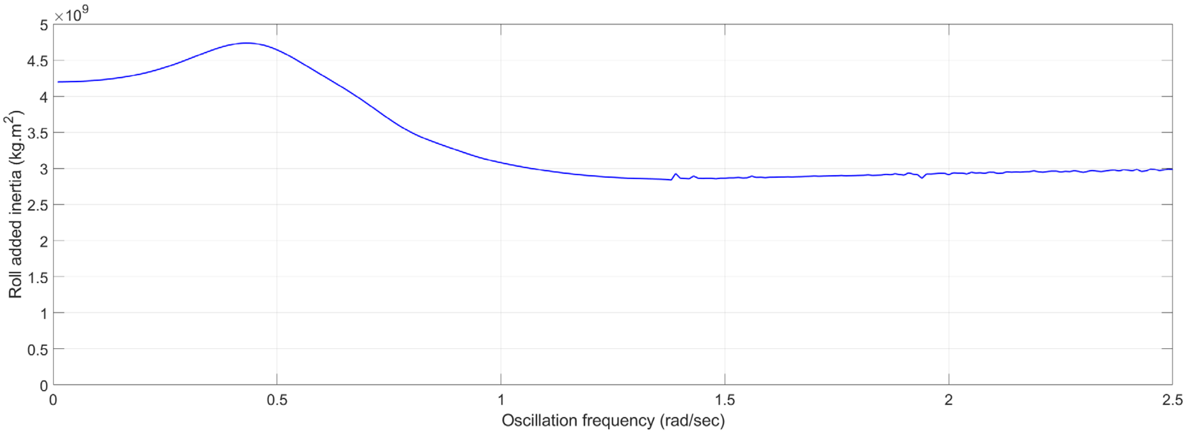


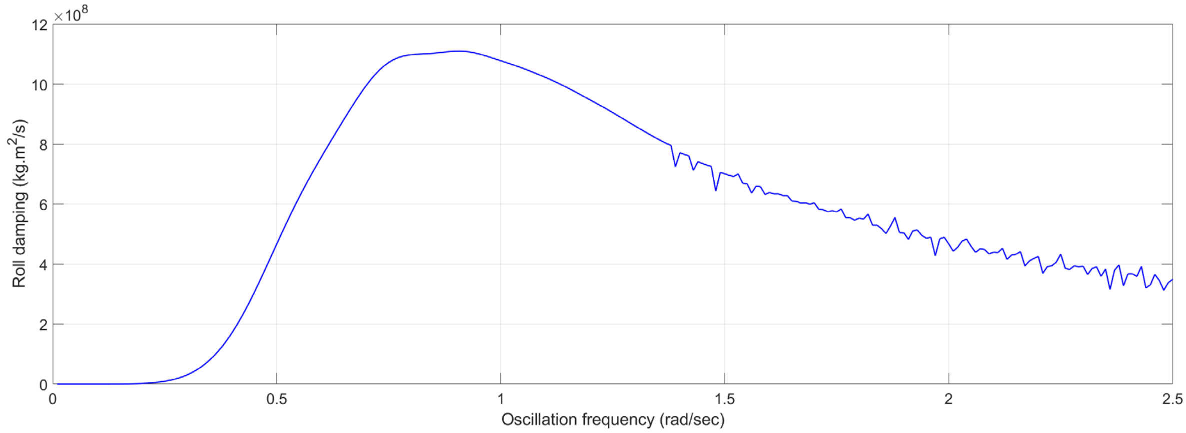


**Figure 12: Roll added inertia (top) and damping (bottom), as calculated using WAMIT**

Roll impulse response is shown in Figure 13.

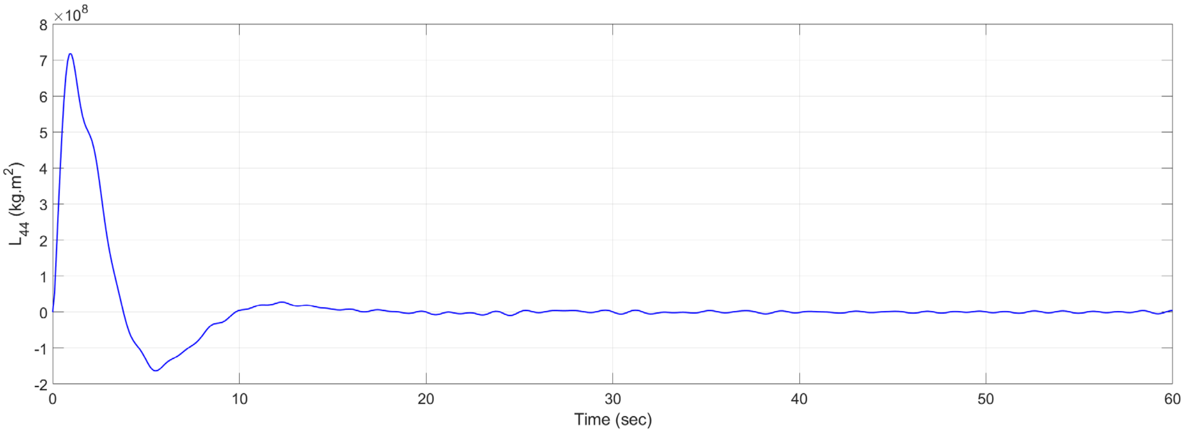


**Figure 13: Roll impulse response function, as calculated using WAMIT**

All other motion components and cross-coupling terms are also included in the analysis.